Infrared Spectra of $H^+(H_2O)_{5-8}$ Clusters: Evidence for Symmetric Proton Hydration

Jyh-Chiang Jiang,[†] Yi-Sheng Wang,[‡] Hai-Chou Chang,[†] Sheng H. Lin,[†,‡] Yuan T. Lee,[†,‡] Gereon Niedner-Schatteburg,[§] and Huan-Cheng Chang*[,†,||]

Contribution from the Institute of Atomic and Molecular Sciences, Academia Sinica, P.O. Box 23-166, Taipei, Taiwan 106, ROC, Department of Chemistry, National Taiwan University, Taipei, Taiwan 106, ROC, and Institut für Physikalische und Theoretische Chemie, Technische Universität München, Lichtenbergstrasse 4, 85747 Garching, Germany

Received January 4, 1999

Abstract: Protonated water clusters, $H^+(H_2O)_n$ ($n = 5-8$), from a supersonic expansion have been investigated by vibrational predissociation spectroscopy and ab initio calculations. The experimental spectra were obtained at an estimated cluster temperature of 170 ± 20 K. Recorded absorption bands at the frequency range of 2700−3900 cm^{-1} are attributed to the free- and hydrogen-bonded-OH stretches of the ion core and the surrounding solvent molecules. Ab initio calculations, performed at the B3LYP/6-31+G* level, indicate that geometries of the $H^+(H_2O)_{5-8}$ isomers are close in energy, with the excess proton either localized on a single water molecule, yielding $H_3O^+(H_2O)_{n-1}$, or equally shared by two molecules, yielding $H_5O_2^+(H_2O)_{n-2}$. Systematic comparison of the experimental and computed spectra provides compelling evidence for both cases. The unique proton-transfer intermediate $H_5O_2^+(H_2O)_4$ was identified, for the first time, by its characteristic bonded-OH stretching absorptions at 3178 cm^{-1}. The existence of five-membered-ring isomers at $n = 7$ is also evidenced by the distinct bonded-OH stretches at 3500−3600 cm^{-1} and by the free-OH stretch of three-coordinated H_2O at 3679 cm^{-1}. Among these $H^+(H_2O)_7$ isomers is a newly discovered $H_5O_2^+$-containing pentagonal ring, which is computed to be lowest in Gibbs free energy at 170 K. Its spectroscopic signature is the splitting of two equivalent bonded OH stretches into a doublet (3544 and 3555 cm^{-1}) by vibrational coupling through ring closure. No profound spectral evidence, however, was found for the formation of four-membered rings although it is predicted to be favorable in terms of total interaction energy for $H^+(H_2O)_7$. Six-membered ring and three-dimensional cagelike structures are also stable isomers but they are less strongly bound. The preference of five-membered-ring formation at $n = 7$ appears to be the result of a delicate balance between entropy and enthalpy effects at the presently investigated cluster temperature. The correlation of this investigation with other studies of neutral water clusters and of the hydration of biological macromolecules is emphasized.

Introduction

Protonated water clusters $[H^+(H_2O)_n]$, undoubtedly, are among the most thoroughly explored cluster ions in the gas phase ever since they were found by mass spectrometry and investigated for collisional proton transfer and ligand exchange reactions. In early 1970s, Kebarle and co-workers[1] pioneered the hydration energy measurements, Newton and Ehrenson[2] performed elaborate calculations, and Schwarz[3] obtained the first infrared absorption spectra of proton hydrates in a cold static cell with a cluster size of $n = 2-4$. In the following decades, studies on the structures and energetics, along with studies of particular ion−molecule reactions,[4] have been actively undertaken owing to the importance of $H^+(H_2O)_n$ in the atmosphere,[5] in solution phases, and in almost any biological systems.[6] They serve to investigate heterogeneous chlorine activation via reactions of surface OH groups as that occurring on polar stratospheric clouds in the context of the seasonal ozone hole over Antarctica.[7] In condensed phases, protonated water clusters have often been employed as a model system for the understanding of proton migration in liquid water[8−10] as well as the transfer of protons through proteins embedded in membranes.[11] Moreover, these gas-phase clusters were shown to act as acidic

[†] Institute of Atomic and Molecular Sciences.
[‡] National Taiwan University.
[§] Technische Universität München.
[||] E-mail: hcchang@po.iams.sinica.edu.tw.

(1) Kebarle, P.; Searles, S. K.; Zolla, A.; Scarborough, J.; Arshadi, M. *J. Am. Chem. Soc.* **1967**, *89*, 6393. Cunningham, A. J.; Payzant, J. D.; Kebarle, P. *J. Am. Chem. Soc.* 1**972**, *94*, 7627.

(2) Newton, M. D.; Ehrenson, S. *J. Am. Chem. Soc.* **1971**, *93*, 4971. Newton, M. D. *J. Chem. Phys.* **1977**, *67*, 5535.

(3) Schwarz, H. A. *J. Chem. Phys.* **1977**, *67*, 5525.

(4) See, for example: Yang, X.; Zhang, X.; Castleman, A. W., Jr. *Int. J. Mass Spectrom. Ion Processes* **1991**, *109*, 339. Honma, K.; Sunderlin, L. S.; Armentrout, P. B. *J. Chem. Phys.* **1993**, *99*, 1623. Choi, J.-H.; Kuwata, K. T.; Haas, B.-M.; Cao, Y.; Johnson, M. S.; Okumura, M. *J. Chem. Phys.* **1994**, *100*, 7153.

(5) Wayne, R. P. *Chemistry of Atmospheres*; Oxford University Press: Oxford, U.K., 1991.

(6) Jeffrey, G. A.; Saenger, W. *Hydrogen Bonding in Biological Structures*; Springer-Verlag: Berlin, 1991.

(7) Nelson, C. M.; Okumura, M. *J. Phys. Chem.* **1992**, *96*, 6112. Schindler, T.; Berg, C.; Niedner-Schatteburg, G.; Bondybey, V. E. *J. Chem. Phys.* **1996**, *104*, 3998.

(8) Tuckerman, M. E.; Laasonen, K.; Sprik, M.; Parrinello, M. *J. Chem. Phys.* **1995**, *103*, 150. Tuckerman, M. E.; Marx, D.; Klein, M. L.; Parrinello, M. *Science* **1997**, *275*, 817. Sagnella, D. E.; Tuckerman, M. *J. Chem. Phys.* **1998**, *108*, 2073. Marx, D.; Tuckerman, M. E.; Hutter, J. G.; Parrinello, M. *Nature* **1999**, *397*, 601.

(9) Lobaugh, J.; Voth, G. A. *J. Chem. Phys.* **1996**, *104*, 2056. Pavese, M.; Voth, G. A. *Ber. Bunsen-Ges. Phys. Chem.* **1998**, *102*, 527. Schmitt, U. W.; Voth, G. A. *J. Phys. Chem. B* **1998**, *102*, 5547.

(10) Vuilleumier, R.; Borgis, D. *J. Mol. Struct.* **1997**, *436*, 555. *Chem. Phys. Lett.* **1998**, *284*, 71; *J. Phys. Chem. B* **1998**, *102*, 4261.

10.1021/ja990033i CCC: $19.00
Published on Web 02/05/2000

microsolvation matrixes, within which acid-catalyzed reactions can occur much like in bulk solution.[12]

Numerous theoretical calculations[2,13−22] concerned the energetics of the association reaction $H^+(H_2O)_{n-1} + H_2O \rightarrow H^+(H_2O)_n$ and the isomeric interconversion between $H_3O^+(H_2O)_{n-1}$ and $H_5O_2^+(H_2O)_{n-2}$. While the protonated water dimer has been treated at all (including the highest available) levels of theory,[13−16] larger clusters were only accessible to reduced or approximated theoretical treatments.[16−21] This was unfortunate as protonated water clusters are presumed to potentially exist either as H_3O^+-centered $[H_3O^+(H_2O)_{n-1}]$ or $H_5O_2^+$-centered $[H_5O_2^+(H_2O)_{n-2}]$ isomers with the extra proton being bound to one or two water molecules, respectively. Which of the above possibilities truly prevails seemed to depend on the structures and solvation numbers of the clusters, but the answer remained largely inconclusive. From early experimental investigations of bulk water, a structure with a closed first solvation shell around an H_3O^+ cation was deduced.[23] Infrared spectra of aqueous acidic solutions, however, were interpreted in terms of a protonated water dimer, $H_5O_2^+$,[24] which is also known to exist in crystal hydrates with a C_2 symmetry.[25] The proof of a conceivable isomerization between the protonated water monomer (sometimes called "Eigen" structure) and the protonated dimer (called "Zundel" cation) and of their temporal coexistence would be of the utmost importance for microscopic understanding of a proposed structural diffusion mechanism (called Grötthuss mechanism) that was established to explain the anomalously high proton mobility in aqueous solutions.[8−10,26]

Despite the fundamental importance of protonated water clusters, the current interpretation of the spectroscopic data of $H^+(H_2O)_n$ has been limited to small sizes of $n = 2-4$,[22] and our understanding of the structures and possible dynamics of larger clusters remained rudimentary. The first infrared spectra of size-selected $H^+(H_2O)_n$, $n = 5-9$, were published by Crofton et al.[27] in 1994, but they failed to come up with a conclusive interpretation of prevailing cluster structures. Wei and Salahub[19] performed ab initio molecular dynamics simulations and attempted to identify possible isomers by comparing the published spectra with their calculations largely under consideration of noncyclic hydrated H_3O^+ clusters as that proposed by Price.[28] The calculated stick diagrams, however, were at considerable variance with the experimentally observed spectra.[19] One of the obvious deviations lies in the observation of the sharp feature at ~3680 cm^{-1}, which cannot be attributed to any of the OH stretches of a noncyclic cluster. Additional unidentified spectral features also exist in the hydrogen-bonded-OH stretching region. These marked disagreements between calculations and observations remained unresolved until now. We started the present reinvestigation[29] of medium- to large-sized protonated homogeneous water clusters only after we have gained new insight from the investigations of hydrated ammonia,[30−32] protonated methanol clusters,[33] and other heterogeneous complexes.[34]

We have demonstrated in the case study of hydrated ammonia clusters, $NH_4^+(H_2O)_n$ ($n = 3-6$),[30−32] that a joint evaluation of vibrational predissociation spectra and high-level ab initio calculations permits an unambiguous determination of structures and isomeric transition temperatures. We identified a number of structural isomers and attributed the observed 3688 cm^{-1} band to the free-OH stretching mode of three-coordinated water molecules involved in a four-membered ring.[30,31] Thanks to the tetrahedral symmetry of the ammonium ion core, which produces a number of remarkably distinct features rarely found in other cluster ions, we are allowed to use $NH_4^+(H_2O)_n$ as a benchmark system for comparison. In addition to the hydrated ammonia clusters, we also studied protonated methanol, $H^+(CH_3OH)_n$,[33] and mixed ether−water, $(CH_3)_2O-H^+-(H_2O)_n$,[34] clusters. These two cluster ions offer the merits of simplicity since the constituents contain hydrophobic methyl groups that effectively block hydrogen bonding. Particularly in the exploration of cyclic $H^+(CH_3OH)_5$,[33] we obtained the first spectroscopic evidence of symmetric proton stabilization between two solvated methanol molecules. Altogether, these three benchmark systems provide a solid basis for the present task of structural identification of the more complex $H^+(H_2O)_{5-8}$ cluster isomers. We expect this identification to help for a better understanding of proton-transfer reactions in aqueous solutions as well as in biological systems at a microscopic level.

Methodologies

A. Ab Initio Calculations. The ab initio calculations, based upon density functional theory (DFT), were performed by using the Gaussian 94 program package.[35] We employed the B3LYP functional together with a standard double-ζ plus polarization basis set, 6-31+G*,[32] which has been augmented with additional diffuse functions for non-hydrogen elements. This combination of method and basis set (B3LYP/6-31+G*) has been successfully applied to protonated ammonia−water clusters[31,32] and neutral benzene−water clusters[36] before. We thus expect it to

(11) Pomès, R.; Roux, B. *J. Phys. Chem.* **1996**, *100*, 2519. Drukker, K.; de Leeuw, S. W.; Hammes-Schiffer, S. *J. Chem. Phys.* **1998**, *108*, 6799.

(12) Achatz, U.; Joos, S.; Berg, C.; Schindler, T.; Beyer, M.; Albert, G.; Niedner-Schatteburg, G.; Bondybey, V. E. *J. Am. Chem. Soc.* **1998**, *120*, 1876.

(13) A recent review concerning the structure of $H_5O_2^+$ has been given by: Xie, Y.; Remington, R. B.; Schaefer, H. F., III. *J. Chem. Phys.* **1994**, *101*, 4878.

(14) Cheng, H.-P.; Krause, J. L. *J. Chem. Phys.* **1997**, *107*, 8461. Cheng, H.-P. *J. Phys. Chem. A* **1998**, *102*, 6201.

(15) Termath, V.; Sauer, J. *Mol. Phys.* **1997**, *91*, 963.

(16) Ojamäe, L.; Shavitt, I.; Singer, S. J. *Int. J. Quantum Chem.* **1995**, *S29*, 657; *J. Chem. Phys.* **1998**, *109*, 5547.

(17) Rahmouni, A.; Kochanski, E.; Wiest, R.; Wormer, P. E. S.; Langlet, J. *J. Chem. Phys.* **1990**, *93*, 6648.

(18) Lee, E. P. F.; Dyke, J. M. *Mol. Phys.* **1991**, *73*, 375.

(19) Wei, D. Q.; Salahub, D. R. *J. Chem. Phys.* **1994**, *101*, 7633; **1997**, *106*, 6086.

(20) Corongiu, G.; Kelterbaum, R.; Kochanski, E. *J. Phys. Chem.* **1995**, *99*, 8038. Kelterbaum, R.; Kochanski, E. *J. Chem. Phys.* **1995**, *99*, 12493.

(21) Hodges, M. P.; Stone, A. J. *J. Chem. Phys.* **1999**, *110*, 6766.

(22) A critical review on this subject has been provided by: Kochanski, E.; Kelterbaum, R.; Klein, S.; Rohmer, M. M.; Rahmouni, A. *Adv. Quantum Chem.* **1997**, *28*, 273.

(23) Eigen, M.; Maeyer, L. D. *Proc. R. Soc. London* **1958**, *A247*, 505. Eigen, M. *Angew. Chem.* **1964**, *3*, 1.

(24) Zundel, G. In *The Hydrogen Bond: Recent Developments in Theory and Experiment*; Schuster, P., Zundel, G., Sandory, C., Eds.; North-Holland: Amsterdam, 1976; Vol. 2, Chapter 15. Danninger, W.; Zundel, G. *J. Chem. Phys.* **1981**, *74*, 2769.

(25) Olovsson, I. *J. Chem. Phys.* **1968**, *49*, 1063. Minkwitz, R.; Schneider, S.; Kornath, A. *Inorg. Chem.* **1998**, *37*, 4662 and references therein.

(26) Agmon, N. *Chem. Phys. Lett.* **1995**, *244*, 456.

(27) Crofton, M. W.; Price, J. M.; Lee, Y. T. In *Clusters of Atoms and Molecules*; Haberland, H., Ed.; Springer-Verlag: Berlin, 1994; pp 45−76.

(28) Price, J. M. Ph.D. Thesis, University of California, Berkeley, CA, 1990; Chapter 2.

(29) Chang, H.-C.; Jiang, J. C.; Wang, Y.-S.; Chang, H.-C.; Lin, S. H.; Lee, Y. T. *J. Chin. Chem. Soc.* **1999**, *121*, 4443.

(30) Wang, Y.-S.; Jiang, J. C.; Cheng, C.-L.; Lin, S. H.; Lee, Y. T.; Chang, H.-C. *J. Chem. Phys.* **1997**, *107*, 9695.

(31) Wang, Y.-S.; Chang, H.-C.; Jiang, J. C.; Lin, S. H.; Lee, Y. T.; Chang, H.-C. *J. Am. Chem. Soc.* **1998**, *120*, 8777.

(32) Jiang, J. C.; Chang, H.-C.; Lee, Y. T.; Lin, S. H. *J. Phys. Chem. A* **1999**, *103*, 3123. The accuracy of the DFT method has been established by this study, where benchmark calculations on $NH_4^+-H_2O$ indicated that both B3LYP and MP2 approaches with the 6-31+G* basis set are well suited for characterizing larger $NH_4^+(H_2O)_n$ clusters.

(33) Chang, H.-C.; Jiang, J. C.; Lin, S. H.; Lee, Y. T.; Chang, H.-C. *J. Phys. Chem. A* **1999**, *103*, 2941. Chang, H.-C.; Jiang, J. C.; Chang, H.-C.; Wang, L. R.; Lee, Y. T. *Isr. J. Chem.*, in press.

(34) Chang, H.-C.; Jiang, J. C.; Hahndorf, I.; Lin, S. H.; Lee, Y. T.; Chang, H.-C. *J. Am. Chem. Soc.* **1999**, *121*, 4443.

describe comparably well the intermolecular hydrogen bonds in protonated water clusters. Geometries of various structural isomers were optimized by analytical gradients. Harmonic vibrational frequencies were obtained from analytical second derivatives and scaled with respect to the experimentally observed free-OH stretches by application of a single scaling factor of 0.973, as used in our previous studies of $NH_4^+(H_2O)_n$ and $CH_3NH_3^+(H_2O)_n$.[30] The choice of this factor,[37] however, often resulted in an underestimation of the frequencies of the hydrogen-bonded-OH stretches involved in a four-membered ring.[31] Therefore, additional calculations using the methods of B3LYP/aug-cc-pVDZ[38] and MP2/6-31+G* were performed on clusters of special interest (with a scaling factor of 0.969 and 0.960, respectively) for further comparison.

We calculated the total interaction energies of $H^+(H_2O)_n$, according to the clustering

$$H_3O^+ + (n-1)H_2O \rightarrow H^+(H_2O)_n$$

for all low-energy isomers of $n = 4-8$. Both zero-point vibrational effects and basis-set superposition errors were corrected to obtain these numbers. As seen from Table 1, the zero-point vibrations have a strong effect in altering the relative stability of these isomers. The effect is particularly noticeable between noncyclic and cyclic isomers, such as **5I** and **5III**, and between H_3O^+-centered and $H_5O_2^+$-centered isomers, such as **6I** and **6II**. Table 2 compares the calculated values to available experimental data[39,40] which are averaged over low-lying isomers without identifying them. A general agreement between calculations and observations is reached. The reasonably good agreement supports the use of the B3LYP/6-31+G* level of computation for description of such hydrogen-bonding systems.

B. Vibrational Predissociation Spectroscopy. Vibrational predissociation spectra of cluster ions were obtained by the use of an ion trap tandem mass spectrometer in combination with a pulsed infrared laser system. Details of the experimental setup have been described elsewhere.[31] Briefly, a corona discharge of 50−200 Torr of H_2 seeded with water vapor synthesized H_3O^+ cations that traveled with the carrier gas flow through the adjacent, continuously operated nozzle. Efficient clustering with neutral water molecules occurred both in the high-pressure region of the nozzle and in the following supersonic expansion. Such jet-synthesized clusters were then extracted, accelerated, and, after size selection by a 60° sector magnet, injected into an octopole ion trap and stored for further usage. A consecutive radio frequency quadrupole mass filter served for product analysis.

In the octopole trap, metastable fragmentation rates of the stored cluster ions were determined to compare with model predictions,[41] which provide rough estimates of the cluster temperatures. At the investigated cluster size of $n = 5-8$, a temperature of about 170 K was obtained. We managed to tune it by ±20 K by adjusting the backing pressure and nozzle temperature for the supersonic expansion. While our estimation involved certain approximations, the obtained temperatures are comparable to the values independently estimated by Schindler et al.[42] for $H^+(H_2O)_n$ of similar sizes when stored in an ion cyclotron resonance cell.

Table 1. Ab-Initio-Calculated Energies (hartree)[a] of $H^+(H_2O)_{4-8}$ Using B3LYP/6-31+G*

species	E	E_{zpve}[b]	E_f[c]
H_2O	−76.422 572 3	−76.401 483	
H_3O^+	−76.691 525 0	−76.657 244	
4I	−306.091 444 6	−305.983 497	−305.976 148
4II	−306.085 881 1	−305.980 185	−305.972 903
4III	−306.085 957 4	−305.976 115	−305.967 889
5I	−382.537 960 8	−382.405 822	−382.396 241
5II	−382.532 645 2	−382.401 374	−382.391 861
5III	−382.539 862 3	−382.405 536	−382.395 073
5IV	−382.533 642 4	−382.399 593	−382.388 982
5V	−382.534 811 4	−382.402 012	−382.391 310
5VI	−382.536 050 2	−382.402 315	−382.391 902
6I	−458.982 664 3	−458.825 967	−458.814 338
6II	−458.981 663 0	−458.827 615	−458.816 000
6III	−458.984 887 7	−458.826 417	−458.813 883
6IV	−458.984 417 6	−458.826 377	−458.813 831
6V	−458.985 830 8	−458.827 088	−458.814 327
6VI	−458.983 284 4	−458.824 883	−458.812 086
6VII	−458.985 420 2	−458.826 539	−458.813 648
7I	−535.425 990 3	−535.245 039	−535.231 407
7II	−535.424 665 3	−535.244 674	−535.230 949
7III	−535.430 057 8	−535.247 077	−535.232 264
7IV	−535.428 973 5	−535.246 530	−535.231 693
7V	−535.428 338 6	−535.244 712	−535.229 637
7VI	−535.428 241 4	−535.248 084	−535.233 315
7VII	−535.426 770 3	−535.243 887	−535.228 799
7VIII	−535.430 752 5	−535.247 243	−535.231 896
7IX	−535.428 664 0	−535.245 618	−535.230 573
7X	−535.429 424 5	−535.246 380	−535.231 451
7XI	−535.428 163 6	−535.245 040	−535.230 428
7XII	−535.425 778 9	−535.242 721	−535.227 635
7XIII	−535.433 515 8	−535.245 836	−535.229 086
7XIV	−535.426 053 2	−535.239 059	−535.222 621
8I	−611.886 613 0	−611.662 155	−611.646 548
8II	−611.872 512 4	−611.667 415	−611.650 334
8III	−611.871 123 4	−611.663 481	−611.645 440
8IV	−611.872 121 0	−611.664 621	−611.647 630
8V	−611.872 820 7	−611.662 317	−611.643 307

[a] 1 hartree = 627.52 kcal/mol. [b] Corrected with zero-point vibrational energies. [c] Corrected with both zero-point vibrational energies and basis-set superposition errors.

Infrared spectra of size-selected water cluster ions were obtained by application of the tunable pulsed laser based on difference frequency generation in $LiNbO_4$.[31] Upon resonant absorption of infrared photons into OH stretches, dissociation took place predominantly via loss of a single water molecule,

$$H^+(H_2O)_n + h\nu \rightarrow H^+(H_2O)_{n-1} + H_2O$$

Vibrational predissociation spectra were resulted from recording the product intensity as a function of laser wavelength. Since the typical stepwise dissociation energy of the clusters sized $n = 5-8$ is ~12 kcal/mol (Table 2), vibrational predissociation can be induced via one-photon absorption (3700 cm^{-1} ~ 11 kcal/mol) at the expense of some internal energy. Lowering the photon energy at some point inevitably decreases the dissociation rate exponentially. The actual limit of detection in this experiment depends on the cluster size and on the largely unknown rate of internal vibrational redistribution. The latter couples the photoexcited vibrations not only to the dissociation-promoting modes but also to the dissipating heat bath of all other unreactive vibrational modes.

Results and Analysis

Figure 1 depicts 3 structural isomers of $H^+(H_2O)_4$ from the present calculations which yield results in accord with previous studies.[2,18,19] A prior measurement[43] indicated that the predomi-

(35) Frisch, M. J.; Trucks, G. W.; Schlegel, H. B.; Gill, P. M. W.; Johnson, B. G.; Robb, M. A.; Cheeseman, J. R.; Keith, T.; Petersson, G. A.; Montgomery, J. A.; Raghavachari, K.; Al-Laham, M. A.; Zakrzewski, V. G.; Ortiz, J. V.; Foresman, J. B.; Cioslowski, J.; Stefanov, B. B.; Nanayakkara, A.; Challacombe, M.; Peng, C. Y.; Ayala, P. Y.; Chen, W.; Wong, M. W.; Andres, J. L.; Replogle, E. S.; Gomperts, R.; Martin, R. L.; Fox, D. J.; Binkley, J. S.; Defrees, D. J.; Baker, J.; Stewart, J. P.; Head-Gordon, M.; Gonzalez, C.; Pople, J. A.; *Gaussian 94, Revision D.3*; Gaussian, Inc.: Pittsburgh, PA, 1995.

(36) Gruenloh, C. J.; Carney, J. R.; Arrington, C. A.; Zwier, T. S.; Fredericks, S. Y.; Jordan, K. D. *Science* **1997**, *276*, 1678.

(37) Since there has been no single universal scaling factors for both free- and bonded-OH stretches, to avoid arbitrary scaling of the calculated harmonic frequencies, we used only one single scaling factor, 0.973, chosen with respect to the highest-frequency free-OH stretches. As found from a series of measurements,[30−34] the typical deviation between observed and such scaled frequencies is less than 10 cm^{-1} for free-OH stretches but is ~50 cm^{-1} for bonded-OH stretches.

(38) Xantheas, S. S. *J. Chem. Phys.* **1995**, *102*, 4505.

(39) Kebarle, P. *Annu. Rev. Phys. Chem.* **1977**, *28*, 445.

(40) Meot-Ner, M.; Speller, C. V. *J. Phys. Chem.* **1986**, *90*, 6616.

(41) Klots, C. E. *Z. Phys. D.* **1991**, *20*, 105.

(42) Schindler, T.; Berg, C.; Niedner-Schatteburg, G.; Bondybey, V. E. *Chem. Phys. Lett.* **1996**, *250*, 301.

Table 2. Experimental and ab-Initio-Calculated Total Energies (kcal/mol) of the Clustering, $H^+(H_2O) + (n-1)H_2O \rightarrow H^+(H_2O)_n$[a]

isomers $H^+(H_2O)_n$	B3LYP/6-31+G*				expt[b]	
	ΔE_n	ΔH_n^{298}	ΔG_n^{298}	ΔG_n^{170}	$\Delta H°_n{}^{298}$	$\Delta G°_n{}^{298}$
4I	−71.8	−73.9	−49.0	−59.7	−68.4, −68.6, −71	−46.9, −46.8, −46
4II	−69.8	−72.0	−47.4	−58.0		
4III	−66.6	−69.8	−41.8	−53.8		
5I	−83.5	−85.9	−53.3	−67.3	−79.9, −81.3, −84	−52.5, −52.5, −51
5II	−80.8	−83.5	−50.6	−64.7		
5III	−82.8	−85.8	−50.9	−65.9		
5IV	−80.8	−84.0	−48.5	−63.8		
5V	−78.9	−82.4	−47.1	−62.3		
5VI	−80.4	−84.0	−47.6	−63.2		
6I	−93.9	−96.9	−56.2	−73.7	−91.0, −92.9, −92	−57.0, −56.6, −54
6II	−95.0	−97.6	−57.6	−74.8		
6III	−93.6	−97.0	−56.4	−73.8		
6IV	−93.6	−96.9	−54.4	−72.7		
6V	−93.9	−97.4	−54.6	−73.0		
6VI	−92.5	−96.1	−53.0	−71.5		
6VII	−93.5	−97.2	−53.4	−72.2		
7I	−103.7	−106.9	−58.8	−79.4	−103.6	−59.6
7II	−103.4	−106.4	−58.5	−79.1		
7III	−104.2	−108.1	−57.7	−79.3		
7IV	−103.9	−107.6	−57.0	−78.7		
7V	−102.6	−106.8	−55.4	−77.5		
7VI	−104.9	−108.4	−58.7	−80.0		
7VII	−102.1	−106.1	−54.5	−77.8		
7VIII	−104.0	−108.2	−56.3	−78.6		
7IX	−103.2	−107.2	−55.7	−76.7		
7X	−103.7	−107.7	−57.0	−78.8		
7XI	−103.1	−107.2	−55.6	−77.7		
7XII	−101.3	−105.6	−53.5	−75.8		
7XIII	−102.3	−108.1	−50.4	−75.1		
7XIV	−98.5	−103.8	−46.8	−71.2		
8I	−112.3	−115.4	−60.5	−84.1		
8II	−114.7	−118.6	−60.6	−85.5		
8III	−111.6	−116.7	−54.9	−81.4		
8IV	−113.0	−117.2	−57.6	−83.2		
8V	−110.2	−116.0	−52.6	−79.8		

[a] Corrected with both zero-point vibrational energies and basis-set superposition errors. [b] See ref 40 for details.

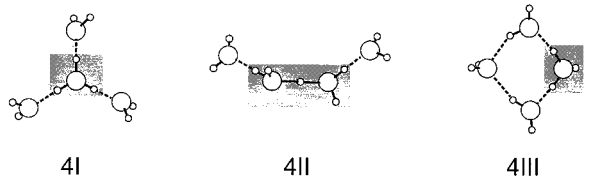

Figure 1. Ab-initio-optimized geometries of $H^+(H_2O)_4$. The O and H atoms are denoted by ○ and ◦, respectively, and the ion core units are gray-shaded for clarity. Note that isomer **4II** contains an incompletely solvated $H_5O_2^+$ ion core; hence, it is ∼2 kcal/mol less stable than the H_3O^+-centered isomer **4I** with a filled first solvation shell.

nant form of $H^+(H_2O)_4$ is the fully hydrated H_3O^+-centered isomer **4I**. The linear $H_5O_2^+(H_2O)_2$ structure (**4II**), containing an excess proton equally shared by two water molecules, is relatively higher in energy (+2 kcal/mol in ΔE_n with respect to **4I**; cf. Table 2), and hence, no spectral evidence was found for this isomer.[43] In a separate experiment of the same research group,[44] the isolated $H_5O_2^+$ cation was concluded to be symmetric (C_2 symmetry) with loss of symmetry (of $H_5O_2^+$ itself becoming C_s symmetry) upon attachment of a weakly interacting ligand, namely H_2. To the best of our knowledge, there has been no unambiguous identification of any symmetric forms of $H_5O_2^+$-centered cluster ions in the gas phase so far.

We recorded the vibrational predissociation spectra of $H^+(H_2O)_n$, $n = 5-8$, in the OH stretching region from 2700 to 3900 cm^{-1} (cf. Figure 2 for an overview). These spectra are primarily identical to that of Price et al.[27,28] but with some significant improvements. One major improvement in the present measurements is that the spectra are better resolved. This improvement in resolution was achieved by lowering the cluster temperature using higher nozzle stagnation pressures. It enabled us to observe, for the first time, weak but characteristic bonded-OH stretching absorption bands in the 3500−3600 cm^{-1} region at $n = 7$. Importantly, the emergence of these spectral features is indicative of structural changeover from noncyclic to cyclic isomers.[45] The individual spectra of $H^+(H_2O)_{5-8}$ are analyzed in comparison to the theoretical predictions as follows.

A. $H^+(H_2O)_5$. Six structural isomers of $H^+(H_2O)_5$ are considered (Figure 3). The open, noncyclic structure **5I** with H_3O^+ as the central ion is computed to be lowest in energy in the present (cf. Tables 1 and 2) as well as in previous studies.[20] This isomer has a filled first solvation shell (1°) around H_3O^+ and a single water molecule situated in the second solvation shell (2°). The linking 1° H_2O molecule is thus involved in two hydrogen bonds. It acts once as a proton acceptor (labeled A) and once as a donor (labeled D), which we designate using the label AD. The second isomer (**5II**), which possesses an unfilled first solvation shell and two 2° H_2O molecules, is ∼3 kcal/mol less stable by comparison. The other three conceivable isomers (**5III**−**5V**), consisting of an H_3O^+ ion core and a four-membered ring, are all higher in energy than the open, noncyclic **5I** by 1−4 kcal/mol. Notably, isomer **5III** is less strongly bound than **5I** by 0.7 kcal/mol; this is opposite to that of $NH_4^+(H_2O)_5$, where

(43) Yeh, L. I.-C.; Okumura, M.; Myers, J. D.; Price, J. M.; Lee, Y. T. *J. Chem. Phys.* **1989**, *91*, 7319. Yeh, L. I.-C.; Lee, Y. T.; Hougen, J. T. *J. Mol. Spectrosc.* **1994**, *164*, 473.

(44) Okumura, M.; Yeh, L. I.; Myers, J. D.; Lee, Y. T. *J. Phys. Chem.* **1990**, *94*, 3416.

(45) The structural changeover resembles that observed for benzene−water clusters (Pribble, R. N.; Zwier, T. S. *Science* **1994**, *265*, 75).

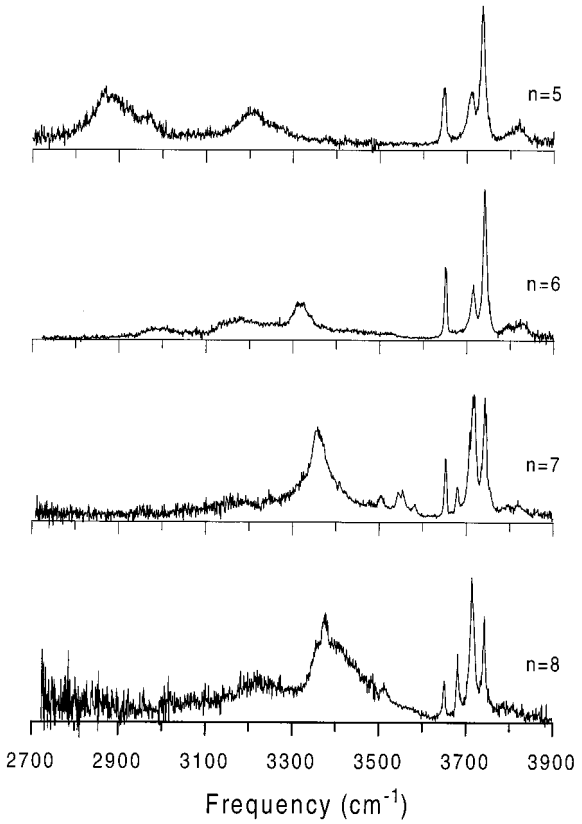

Figure 2. Vibrational predissociation spectra of $H^+(H_2O)_n$, $n = 5-8$, in the OH stretching region. All the spectra are laser power-normalized. Note the emergence of new features at 3500−3600 cm^{-1} from $n = 6$ to 7.

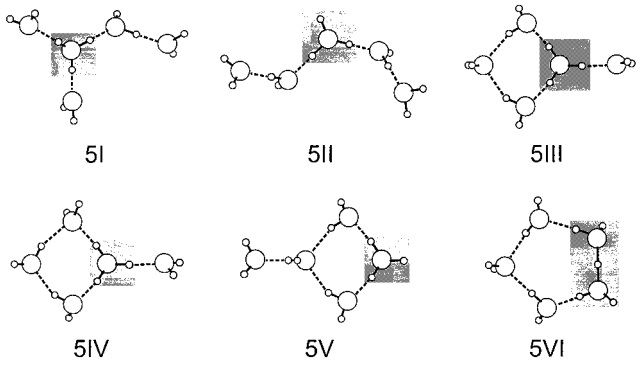

Figure 3. Ab-initio-optimized geometries of $H^+(H_2O)_5$. The O and H atoms are denoted by ○ and ◦, respectively, and the ion core units are gray-shaded for clarity.

the symmetric four-membered ring is the lowest-energy structure.[31,32] We have also computationally explored the possibility of having four water molecules situated in the first solvation shell.[17] This isomer, with the fourth 1° H_2O molecule donating one of its protons to the electron lone pair of H_3O^+, was not found and, therefore, is not included in the present discussion.

Detailed structural analysis of isomer **5I** reveals that the hydronium ion and the first-shell water molecules are connected in a linear O−H$^+$−O configuration, with an angle of ∠O−H$^+$···O = 179°. The local C_2 axis of H_2O is largely collinear with the hydrogen bond, as the interaction between H_3O^+ and 1° H_2O is dominated by charge-dipole attraction. For the bonding between 1° H_2O and 2° H_2O, however, it is primarily governed by the interaction of the 1° H_2O dipole with one of the two oxygen electron lone pairs of the 2° H_2O molecule. Similar intermolecular forces operate in isomer **5III**, where the 2° H_2O acts as a double proton acceptor (AA), forming two equivalent O−H···O hydrogen bonds with the two 1° H_2O(AD) molecules. In this structure, the angle included by the two OH bonds of H_3O^+ is tightened by 6° with respect to that in isomer **5I** due to the strain caused by the four-membered ring formation. Resembling the corresponding feature of $NH_4^+(H_2O)_5$,[31,32] the asymmetric ring isomer **5IV** is higher in energy than **5III** by ∼2 kcal/mol. Isomer **5V**, with an unfilled first solvation shell, is least stable among the three four-membered ring forms. Also considered in Table 2 and Figure 3 is the five-membered-ring isomer (**5VI**), which contains an incompletely solvated $H_5O_2^+$ ion core.[20] Notably, the formation of both four- and five-membered rings (**5III**−**5VI**) in $H^+(H_2O)_5$ is not energetically favored by entropy effects at the given cluster temperature of 170 K (Table 2).[46]

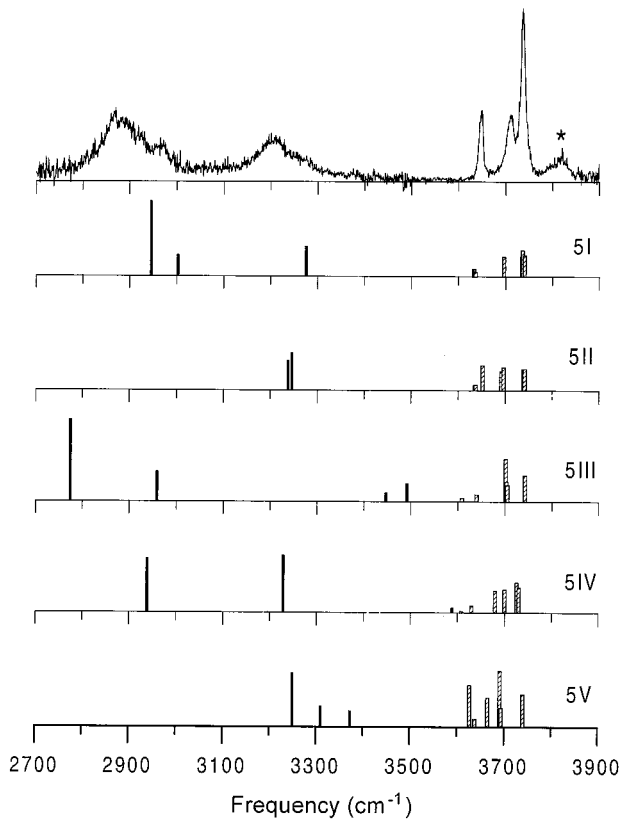

Figure 4. Vibrational predissociation spectrum of $H^+(H_2O)_5$ in the OH stretching region. The beam was expanded at a nozzle temperature of 300 K and a backing pressure of 100 Torr. Shown underneath are the ab-initio-calculated stick diagrams of OH stretches for isomers collected in Figure 3. Note that the intensities of free-OH stretches (▨) have been amplified by a factor of 5 for clearer comparison with those of bonded-OH stretches (■). The asterisk denotes H_2O combination bands.[43]

Comparison of the experimental spectrum of $H^+(H_2O)_5$ with the ab-initio-calculated stick diagrams of isomers **5I**−**5V** clearly favors identification of structure **5I** in this experiment (cf. Figure 4). To further confirm the assignment, we changed the cluster temperature by varying the beam expansion conditions over a wide range; however, only minor differences were found in the spectrum. From this temperature-dependence measurement, it is concluded that the spectrum displayed in Figure 4 should be free of contributions from other isomers.[31] Table 3 presents the detailed spectral assignments of the free-OH stretches resonant

(46) The entropy effect could be underestimated for the open, noncyclic structures since the H_2O(A) molecules are nearly free rotors along their local C_2 axes.

Table 3. Frequencies (cm^{-1}) and Assignments of the Prominent Features Observed in the OH Stretching Spectra of $H^+(H_2O)_{5-8}$

species	freq	isomers[a]	assgnts[b]
$H^+(H_2O)_5$	3817	**5I**	free OH combination bands of 1° or 2° H_2O(A)
	3736	**5I**	asymmetric free OH of 1° or 2° H_2O(A)
	3709	**5I**	free OH of 1° H_2O(A)-A
	3647	**5I**	symmetric free OH of 1° or 2° H_2O(A)
	3208	**5I**	bonded OH of 1° H_2O(AD)-A
	2967	**5I**	asymmetric bonded OH of H_3O^+-A
	2879	**5I**	symmetric bonded OH of H_3O^+-A
$H^+(H_2O)_6$	3817	**6I**, **6II**	free OH combination bands of 1° or 2° H_2O(A)
	3741	**6I**, **6II**	asymmetric free OH of 1° or 2° H_2O(A)
	3713	**6I**	free OH of 1° H_2O(AD)-A
	3651	**6I, 6II**	symmetric free OH of 1° or 2° H_2O(A)
	3320	**6I**	bonded OH of 1° H_2O(AD)-A
	3178	**6II**	bonded OH of $H_5O_2^+$-A
	2988	**6I**	bonded OH of H_3O^+-A
$H^+(H_2O)_7$	3791	**7I**−**7IV**, **7VI**, **7VIII**, **7X**	free OH combination bands of 1° or 2° H_2O(A)
	3742	**7I**−**7IV**, **7VI**, **7VIII**, **7X**	asymmetric free OH of 1° or 2° H_2O(A)
	3717[c]	**7X**	free OH of 2° H_2O(AD)-A
	3710[c]	**7I**−**7IV**, **7VI**, **7VIII**, **7X**	free OH of 1° H_2O(AD)-A
	3679	**7IV**, **7VIII**	free OH of 2° H_2O(AAD)-A
	3652	**7I**−**7IV**, **7VI**, **7VIII**, **7X**	symmetric free OH of 1° or 2° H_2O(A)
	3581	**7X**	bonded OH of 2° H_2O(AD)-AA
	3555[c]	**7VI**	asymmetric bonded OH of 1° H_2O(AD)-AA
	3544[c]	**7VI**	symmetric bonded OH of 1° H_2O(AD)-AA
	3502	**7IV**, **7VIII**, **7X**	bonded OH of 2° H_2O(AD)-AAD or 2° H_2O(AD)-AA
	3360	**7I**−**7IV**, **7VI**, **7VIII**, **7X**	bonded OH of 1° H_2O(AD) or $H_5O_2^+$
	3198	**7I**−**7IV**, **7VI**, **7VIII**, **7X**	bonded OH of 1° H_2O(AD), H_3O^+ or $H_5O_2^+$
$H^+(H_2O)_8$	3781	**8II**[d]	free OH combination bands of 1° or 2° H_2O(A)
	3743	**8II**[d]	asymmetric free OH of 1° or 3° H_2O(A)
	3715	**8II**[d]	free OH of 1° H_2O(AD)-A
	3683	**8II**[d]	free OH of 2° H_2O(AAD)-A
	3652	**8II**[d]	symmetric free OH of 1° or 3° H_2O(A)
	3409	**8II**[d]	bonded OH of 1° H_2O(AD)-AAD
	3373	**8II**[d]	bonded OH of 1° H_2O(AD)-AAD
	3219	**8II**[d]	bonded OH of 2° H_2O(AAD)-A

[a] Isomeric structures illustrated in Figures 1, 3, 5, 8, and 11. [b] The abbreviations used to describe the forms of hydrogen bonding are the following: single-acceptor (A); double-acceptor (AA); single-acceptor−single-donor (AD); double-acceptor−single-donor (AAD). The letter(s) after the dash line represent the perturbation to the assigned molecule.[31] [c] Obtained after deconvolution. [d] Tentative assignments.

at 3647, 3709, and 3736 cm^{-1} and the hydrogen-bonded-OH stretches resonant at 2879, 2967, and 3208 cm^{-1} for this lowest-energy isomer **5I**.

At first glance, the relative absorption intensities of the free- and bonded-OH stretches seem to be at variance between experiment and theory (Figure 4 and others). However, the OH stretching modes, when involved in a hydrogen bond, are well-known not only to red-shift but also to broaden considerably with respect to the free-OH stretching bands.[47] Relative experimental intensities that are integrated over an entire band compare much more favorably with the theoretical predictions, which are void of this broadening.

B. $H^+(H_2O)_6$. The B3LYP/6-31+G* calculations revealed more than 7 low-energy isomers for $H^+(H_2O)_6$, as illustrated in Figure 5. Surprisingly, the H^+-centered isomer **6II**, which might be expected to be a proton transfer intermediate, is actually predicted to be lowest in energy among those structures. It is about 1 kcal/mol more stable than the noncyclic (**6I**) and the cyclic (**6III**−**6VII**) isomers, all comprising an H_3O^+ core ion, mainly due to zero-point vibrational effects (Tables 1 and 2). In addition to the four-membered rings (**6III**−**6VI**), the five-membered-ring structure (**6VII**) is also stable. The relative stability of them follows the order of **6V** > **6III** > **6VII** > **6VI**, a trend closely resembling their structural analogues of $NH_4^+(H_2O)_6$.[31,32] As in the case of $H^+(H_2O)_5$, the formation of either four- or five-membered rings is energetically unfavorable owing to the entropy effect at 170 K (cf. Table 2).

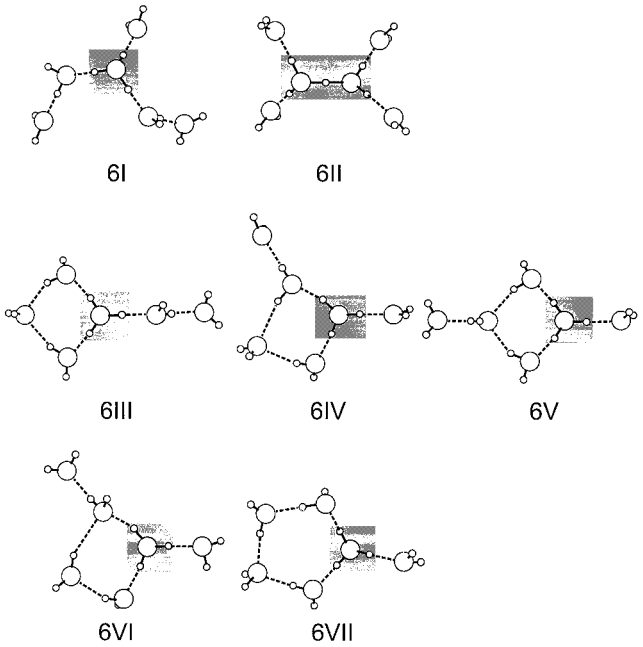

Figure 5. Ab-initio-optimized geometries of $H^+(H_2O)_6$. The O and H atoms are denoted by ○ and ◦, respectively, and the ion core units are gray-shaded for clarity.

Figure 6 displays the OH stretching spectrum of $H^+(H_2O)_6$ and its comparison with the ab-initio-calculated stick diagrams of isomers **6I**−**6VI**. The observed transitions can be separated into two groups: the free-OH stretches at 3651, 3713, and 3741

(47) Pimentel, G. C.; McClellan, A. L. *The Hydrogen Bond*; Freeman: San Francisco, CA, 1960.

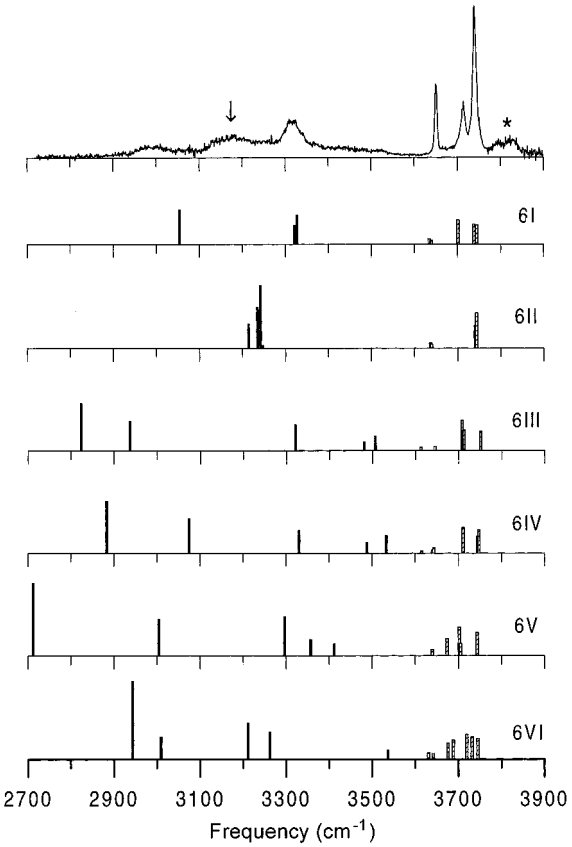

Figure 6. Vibrational predissociation spectrum of $H^+(H_2O)_6$ in the OH stretching region. The beam was expanded at a nozzle temperature of 250 K and a backing pressure of 160 Torr. Shown underneath are the ab-initio-calculated stick diagrams of OH stretches for isomers collected in Figure 5. Note that the intensities of free-OH stretches (⍁) have been amplified by a factor of 5 for clearer comparison with those of bonded-OH stretches (■). The asterisk and the arrow denote H_2O combination bands[43] and the spectral signature of $H_5O_2^+(H_2O)_4$, respectively.

cm^{-1} and the bonded-OH stretches at 2988, 3178, and 3320 cm^{-1}. This spectral pattern is generally similar to that of $H^+(H_2O)_5$ except that (1) a new feature emerges at 3178 cm^{-1} and (2) the 3320 cm^{-1} band is more intense than its partner at 2988 cm^{-1}. There is no free-OH stretching absorption of three-coordinated H_2O at ~3680 cm^{-1}, leading to the conclusion that the four-membered-ring isomers **6V** and **6VI** did not form in the ion source. This lack of ring formation is rationalized by the entropy effect, which also hinders the formation of **6IV** and **6VII** at the cluster temperature of 170 K. It is likely that isomer **6III** is present in the beam, but its existence cannot be fully verified since no distinct bonded-OH stretching absorption features are found at ~3500 cm^{-1}.[31]

The remaining isomers that are not excluded yet are the two open, noncyclic structures (**6I** and **6II**), both of which happen to be favored enthalpy- and entropywise (cf. Table 2). It thus seems justified to attempt an assignment of the experimental spectrum of $H^+(H_2O)_6$ to these two isomers. The assignment is made possible by comparison of the observed spectrum with the computed diagrams of B3LYP/6-31+G* and B3LYP/aug-cc-pVDZ (Figure 7) and with the experimental spectra of three closely related systems: $H^+(H_2O)_5$; $H^+(H_2O)_4(CH_3)_2O$; $H^+(H_2O)_4(C_2H_5)_2O$.[34]

We compare in Table 4 the bonded-OH stretching frequencies of isomers **5I**, $H_3O^+(H_2O)_3[(CH_3)_2O]$, **6I**, and $H_3O^+(H_2O)_3[(C_2H_5)_2O]$, which share the common structure of $H_3O^+(H_2O)_3X$

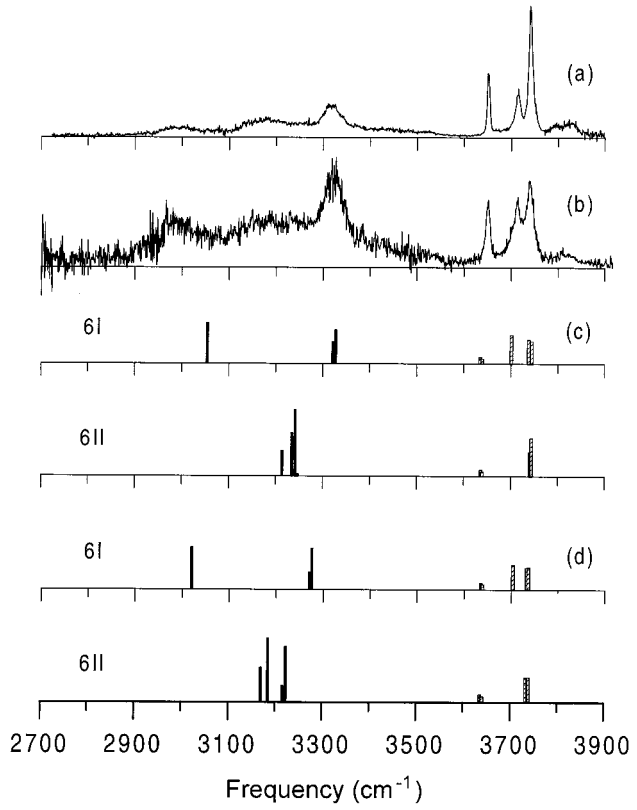

Figure 7. Temperature dependence of the vibrational spectrum of $H^+(H_2O)_6$ in the OH stretching region. The beam was expanded at a (nozzle temperature, backing pressure) of (a) (250 K, 90 Torr) and (b) (310 K, 60 Torr). All the spectra are laser power-normalized. Shown underneath are the ab-initio-calculated stick diagrams of isomers **6I** and **6II** using the (c) B3LYP/6-31+G* and (d) B3LYP/aug-cc-pVDZ methods with the intensities of free-OH stretches (⍁) amplified by a factor of 5 for clearer comparison to those of bonded-OH stretches (■).

Table 4. Correlation of the Proton Affinity (PA) of Ligand X with the Observed Bonded-OH Stretching Frequencies (ν_b) of $H_3O^+(H_2O)_3X$[a]

	X			
	H_2O	$(CH_3)_2O$	$(H_2O)_2$	$(C_2H_5)_2O$
PA (kcal/mol) of X	165.2	189.3	193.2	198.0
ν_b (cm^{-1}) of $H_3O^+(H_2O)_3X$	2879, 2967	2995	2988[b]	3028
	3208	3316	3320[b]	3340

[a] Reference 34 and with the following structure for $H_3O^+(H_2O)_3X$. [b] Of isomer **6I**.

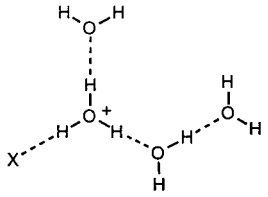

(Table 4) with X = H_2O, $(CH_3)_2O$, $(H_2O)_2$, and $(C_2H_5)_2O$. As previously demonstrated for $H_3O^+(H_2O)_3(H_2O)$, $H_3O^+(H_2O)_3[(CH_3)_2O]$, and $H_3O^+(H_2O)_3[(C_2H_5)_2O]$,[34] the frequency red-shifts of the bonded-OH stretches of both 1° H_2O(AD) and H_3O^+ in these clusters are strongly correlated with the proton affinity of the interacting ligand, X. Table 4 indicates that such a correlation is nearly linear, suggesting that the bonded-OH stretches of **6I** should be similar in frequency to those of $H_3O^+(H_2O)_3[(CH_3)_2O]$ since the proton affinity of the water dimer $(H_2O)_2$ is higher than that of $(CH_3)_2O$ by only 4 kcal/mol. This prediction is indeed verified by the present experiment, as shown

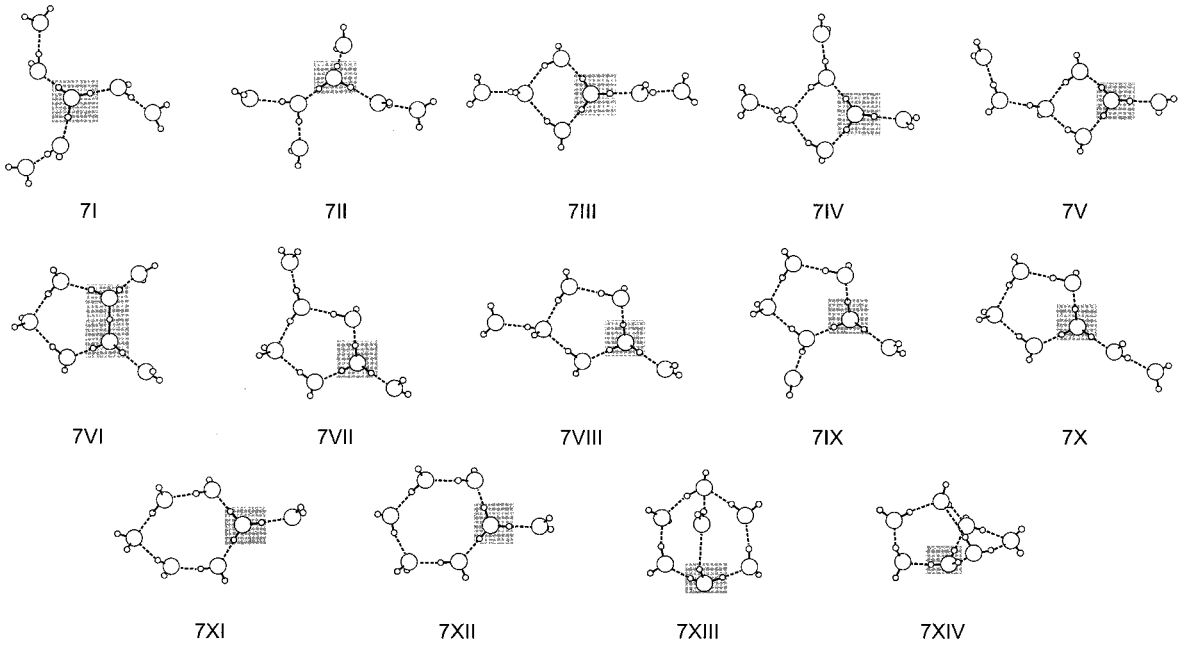

Figure 8. Ab-initio-optimized geometries of $H^+(H_2O)_7$. The O and H atoms are denoted by ○ and ◦, respectively, and the ion core units are gray-shaded for clarity.

in Table 4. The large frequency changes (up to 112 cm^{-1}) of the bonded-OH stretches in going from **5I** to **6I** can, hence, be understood as a result of charge rearrangement due to substantial proton affinity increase of the first-shell water in these clusters.[34] The similarity in the experimental spectra of $H_3O^+(H_2O)_3$-$[(H_2O)_2]$ and $H_3O^+(H_2O)_3[(CH_3)_2O]$ provides a firm and strong support to the assignment of the 2988 and 3320 cm^{-1} bands to the bonded-OH stretches of H_3O^+ and 1° H_2O(AD), respectively, in isomer **6I**.

We are led to make a possible assignment of the new band at 3178 cm^{-1} to isomer **6II**. This band lies halfway between the bonded-OH stretching absorptions of H_3O^+ (at 2988 cm^{-1}) and 1° H_2O (at 3320 cm^{-1}).[48] The intermediate red-shift reflects an intermediate perturbation of the acting OH group by its intra- or intermolecular environment. We note that the considerable difference in red-shift of more than 100 cm^{-1} cannot be accounted for by some minor effects but has to be associated with some strong environmental impact, namely, from the naked charge. The situation intermediate to the two extreme cases of one extra charge per molecule (H_3O^+) and none (H_2O) is when a charge is shared by two neutral water molecules ($H_5O_2^+$). The assignment of the 3178 cm^{-1} band to the bonded-OH stretching modes of $H_5O_2^+$ is thus well justified, and its occurrence in the computed spectra of isomer **6II** (cf. Figures 6 and 7) is comprehensible. The assignments of other associated absorption bands in this spectrum are given in Table 3.

Further support to the assignment of the 3178 cm^{-1} band to isomer **6II** is given by a comparison with the generally similar spectrum of $H^+(H_2O)_5$ (Figure 5). One noticeable result of this comparison is that the absorption band at 3713 cm^{-1} of the free-OH stretch of $H^+(H_2O)_6$ is relatively weaker than that of H^+-$(H_2O)_5$ (cf. Figures 6 and 4, respectively). This is particularly evident when it is compared to the symmetric and asymmetric stretches of the single-acceptor (A) H_2O molecules at ∼3650 and ∼3740 cm^{-1}, respectively. It is noteworthy that the $H_5O_2^+$-$(H_2O)_4$ cluster (**6II**) is the only low-energy isomer that lacks any two-coordinated H_2O. Observations of this band weakening in going from $n = 5$ to $n = 6$, thus, provide an independent support for the presence of this unique isomer (at the expense of isomer **6I**) in the beam. Altogether, there is strong and conclusive evidence for the existence of the $H_5O_2^+$-centered isomer **6II** in the supersonic expansion.

We have also reexamined the above assignments in terms of two structural isomers by tuning the cluster temperature and searching for spectral changes. Figure 7 displays the spectra obtained at different nozzle temperatures and beam expansion conditions with the clusters in part (a) significantly colder than the clusters in part (b). It shows the trend that as the beam temperature increases, the free-OH stretch of 1° H_2O(AD) at 3713 cm^{-1} gains intensity, whereas the bonded-OH stretching absorption at 3178 cm^{-1} diminishes. These spectral changes correspondingly indicate the presence of a lower-energy and a higher-energy isomer, in good agreement with the proposed assignment. That isomer **6II** is more abundant in a colder beam is in correlation with the energetics calculations (Table 2) which predict **6II** to be lowest in energy of all $H^+(H_2O)_6$ isomers collected in Figure 5. The comprehensive evidence for the existence of isomer **6II** permits, for the first time, an unambiguous identification of a hydrated $H_5O_2^+$ ion as a cluster in the gas phase.

C. $H^+(H_2O)_7$. As the cluster increases in size, the number of low-lying isomers exponentially increases and, furthermore, their energy differences diminish with n.[49] A combinatorial study of the $n = 7$ clusters reveals 14 conceivable isomers (cf. Figure 8). This large number of isomers manifests the complex structural isomerism involved in medium-sized protonated water clusters. There are two open noncyclic structures (**7I** and **7II**), three four-membered rings (**7III**−**7V**), five five-remembered rings (**7VI**−**7X**), two six-membered rings (**7XI** and **7XII**), and two three-dimensional cagelike forms (**7XIII** and **7XIV**). Figures 9 and 10 display the experimental infrared spectra in comparison with the computed diagrams of isomers under consideration.

One can derive part of the heptamer structures by starting with the hexamers in mind and attaching one extra water

(48) The other two bonded-OH stretching modes of the H_3O^+ ion core in **6I** were computed to situate at the frequencies of 2463 cm^{-1} (symmetric) and 2609 cm^{-1} (asymmetric), which are beyond the reach of the present laser system.

(49) Berry, R. S. *Chem. Rev.* **1993**, *93*, 2379 and references therein.

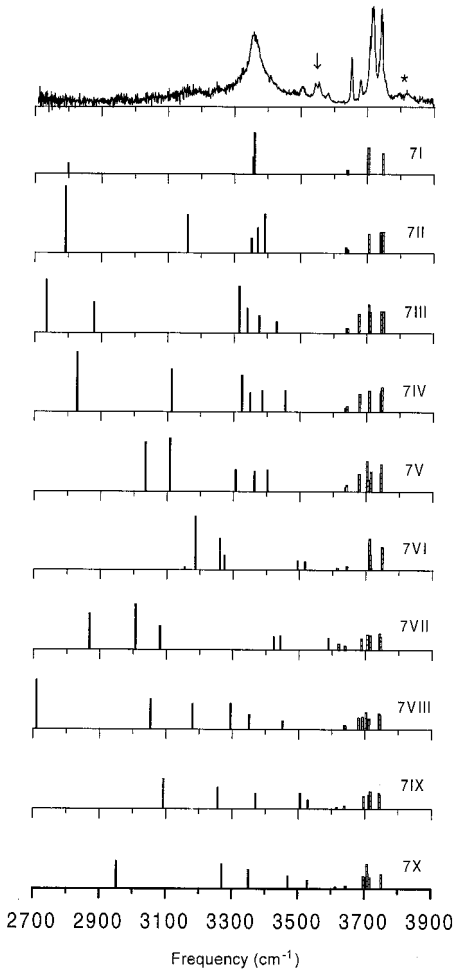

Figure 9. Vibrational predissociation spectrum of $H^+(H_2O)_7$ in the OH stretching region. The beam was expanded at a nozzle temperature of 250 K and a backing pressure of 80 Torr. Shown underneath are the ab-initio-calculated stick diagrams of OH stretches for isomers collected in Figure 8. Note that the intensities of free-OH stretches (⍁) have been amplified by a factor of 5 for clearer comparison with those of bonded-OH stretches (■). The asterisk and the arrow denote H_2O combination bands[43] and the spectral signature of $H_5O_2^+(H_2O)_5$, respectively.

molecule to various possible binding sites. Structure **6I**, for example, can give rise to the noncyclic isomers **7I** and **7II**, and the four-membered rings (**7III**−**7V**) can form by attaching one more H_2O to **6V**. These heptamers are all close in energy to within 2 kcal/mol. Among the five-membered-ring structures (**7VI**−**7X**), isomer **7VI** was computed to be minimum in energy for all $H^+(H_2O)_7$ clusters presently considered. Note that **7VI** builds around an $H_5O_2^+$-core ion, in parallel to **6II** which is also the lowest-energy isomer of the hexamers (Figure 5). The other characteristics of this 5-fold ring family are that (1) isomer **7VIII** contains a three-coordinated H_2O in the form of a double proton acceptor and a single donor (AAD), (2) isomer **7X**, composed of an unperturbed five-membered ring on the solvent side, has an H_2O(AA) located on the second solvation shell, and (3) both isomers **7VII** and **7IX** contain a three-coordinated H_2O molecule concurrently acting as a single proton acceptor and a double donor (ADD), instead of AAD, a feature which is not energetically favored.[32]

The experimentally obtained spectrum of $H^+(H_2O)_7$ is compared to the calculated diagrams of isomers **7I**−**7X** in Figure 9. Four absorption bands fall within the free-OH stretching region above 3600 cm^{-1}. Three of them, namely at 3652, 3717, and 3742 cm^{-1}, also appear in the spectrum of the hexamer. The additional feature at 3679 cm^{-1} is characteristic for the free-OH stretching of a three-coordinated H_2O(AAD), as discussed in our recent investigations.[30,31] Its occurrence is indicative of ring formation. The identification of this peak is one of the achievements with respect to the prior study,[27,28] where it had been observed but could not be unambiguously assigned.

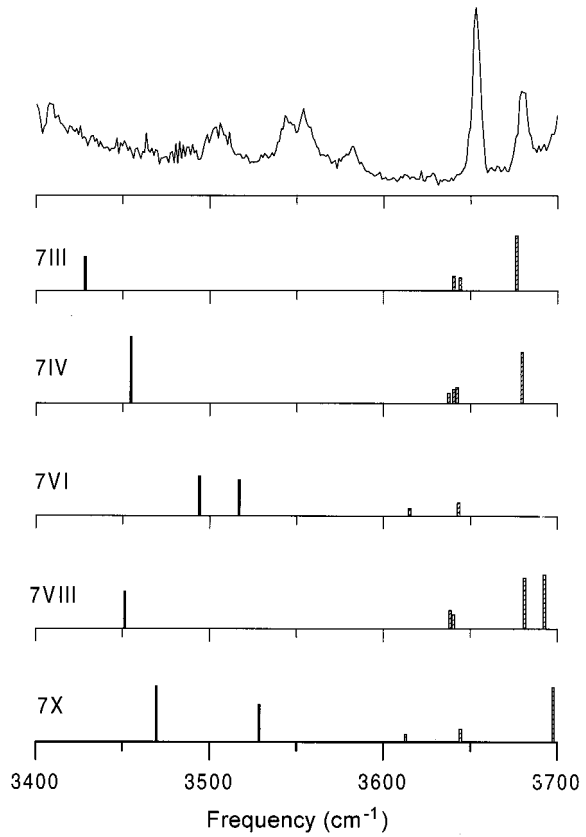

Figure 10. Enlarged view of the OH stretching spectrum of $H^+(H_2O)_7$ and comparison with the ab-initio-calculated stick diagrams using B3LYP/6-31+G* for isomers **7III**, **7IV**, **7VI**, **7VIII**, and **7X**.

Previously,[27,28] the 3500−3600 cm^{-1} frequency region of protonated water clusters was considered to be void of distinct and sharp absorption bands. The present heptamer spectrum reveals four sharp transitions at 3502, 3544, 3555, and 3581 cm^{-1} for the first time. They can be observed only under conditions of supersonic expansion that ensures production of sufficiently cold clusters. The observed bandwidths of only ∼10 cm^{-1} (full width at half-maximum, fwhm) markedly differ than the breadths (fwhm ∼ 100 cm^{-1}) of the lower-lying absorption bands at 3198 and 3360 cm^{-1}. It is comprehensible that less broadening and smaller red-shifts are both related to less softening of the OH stretching mode by hydrogen bonding. Such a possible instance is seen[31] when the affected OH unit (a donor) is bonded to an acceptor that also acts as an acceptor for the second H_2O. Close inspection of the computed structures reveals that such double-acceptor (AA) molecules act as the closing link in ring isomers. Among these four features, the absorption doublet at 3544 and 3555 cm^{-1} (cf. Figure 10) is so remarkably similar in frequency to those (3551 and 3562 cm^{-1})[31] of $NH_4^+(H_2O)_5$ that it can be assigned to the two bonded-OH stretching modes perturbed by the 2° H_2O(AA) in isomer **7VI**. The present calculations predict a stretching doublet of 3494 and 3517 cm^{-1} for these two vibrations. As previously found for $NH_4^+(H_2O)_{3-6}$,[31] the B3LYP/6-31+G* calculations after application of the scaling

factor of 0.973 tend to underestimate the stretching frequencies of bonded-OH groups involved in a ring by ~40 cm^{-1}. This underestimation agrees qualitatively with the presently observed deviation of 50 and 38 cm^{-1} for the low- and high-frequency components, respectively. Dedicated MP2 calculations also yield scaled frequencies of 3514 and 3551 cm^{-1}, in qualitative accord with the measurements. Interestingly, the experimentally observed splitting of 11 cm^{-1} is better reproduced by the B3LYP calculation (23 cm^{-1}) than by the MP2 result (37 cm^{-1}).

The second feature that can be clearly identified in the bonded-OH stretching region is the 3581 cm^{-1} band. It is highest in frequency among the four new peaks and therefore, this vibrational mode must be least perturbed. The most probable isomer that can have a bonded-OH stretch with a frequency even higher than that of **7VI** is **7X**. The B3LYP/6-31+G* (and the MP2/6-31+G*) calculations forecast that the highest and the second-highest frequencies of the three bonded-OH stretches within the unperturbed 5-fold ring of **7X** lie at 3529 (3552) and 3470 (3504) cm^{-1}. The former agrees well with the experimentally observed absorption at 3581 cm^{-1} when the above-mentioned systematic underestimation in the DFT calculation is taken into account. The latter correlates well with the lowest-lying sharp peak at 3502 cm^{-1}. Figure 10 compares in detail the experimentally observed spectrum with the calculated diagrams of isomers **7VI** and **7X**, along with others. In summary, we take the assignments of these four sharp peaks to isomers **7VI** and **7X** as evidence for their formation in the supersonic expansion and for their presence in the ion trap.

The appearance of the 3679 cm^{-1} band, ascribed to the free-OH stretching mode of a three-coordinated H_2O(AAD), is indicative of either four- or five-membered-ring formation. A similar conclusion has been previously reached in the investigations of $NH_4^+(H_2O)_n$ and $CH_3NH_3^+(H_2O)_n$.[30,50] Note that in the protonated water heptamer, all three four-membered-ring isomers (**7III**−**7V**) contain a three-coordinated H_2O. Among the five-membered-ring isomers, only structure **7VIII** has a three-coordinated H_2O. The calculated frequencies of the free-OH stretches of **7III**, **7IV**, and **7VIII** are 3676, 3679, and 3681 cm^{-1}, respectively, all in close agreement with the experimentally observed frequency of 3679 cm^{-1}. To further distinguish these three isomers, the absorptions of other bonded-OH stretching modes are examined. For isomer **7VIII**, the highest-frequency mode of the four bonded-OH stretches of the solvent water molecules is calculated by B3LYP/6-31+G* (MP2/6-31+G*) to be 3451 (3496) cm^{-1}. This frequency is significantly higher than that calculated for isomer **7III** by 20 cm^{-1} but close to that of **7IV** within 5 cm^{-1}. The present experiment reveals a distinct bonded-OH absorption at 3502 cm^{-1}; the absorption is likely to be composed of two superimposed bands, one from isomer **7VIII** or **7IV** and another from **7X** as discussed above. The band superposition is evidenced by the increased width (fwhm) of this feature which is nearly twice as broad as the neighboring 3581 cm^{-1} band. Figure 10 exhibits the comparison between calculations and observations, which clearly supports the attribution of this 3502 cm^{-1} band to isomer **7VIII** or **7IV** rather than to **7III**.

Table 3 presents detailed assignments of the observed spectral features to various OH stretches of isomers **7IV**, **7VI**, **7VIII**, and **7X**. However, the possibility for the presence of **7I** and **7II** in the detection region cannot be ruled out since they are low in energy as well (Table 2). It is difficult to identify these isomers which show no fingerprint absorptions above 3500 cm^{-1}. All vibrational features observed in the frequency region below 3500 cm^{-1} are broad and lack any fine structures. Thus, they provide little-to-no structural information.

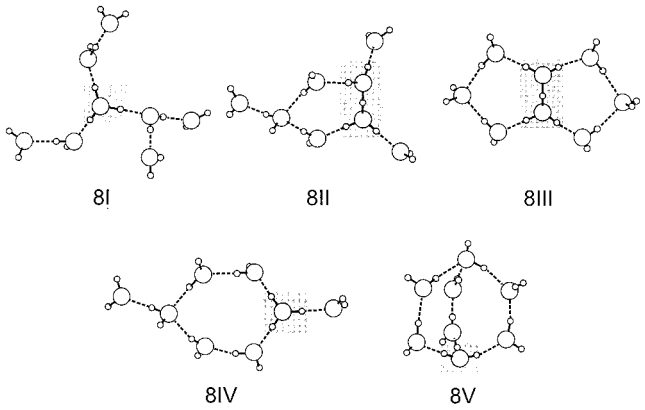

Figure 11. Ab-initio-optimized geometries of $H^+(H_2O)_8$. The O and H atoms are denoted by ○ and ◦, respectively, and the ion core units are gray-shaded for clarity.

D. $H^+(H_2O)_8$. For clusters with a size of $n > 7$, the structural identification becomes exceedingly difficult because a much larger number of isomers is needed to be computationally investigated. The same difficulty arises on the experimental side where there are less distinct vibrational features to be identified owing to spectral congestion. Tables 1 and 2 list the computed energetics of five representative isomers of $H^+(H_2O)_8$ whose structures are illustrated in Figure 11. Among them, the $H_5O_2^+$-containing five-membered-ring structure **8II** is lowest in energy. It is ~3 kcal/mol more strongly bound than isomer **8III** which consists of an $H_5O_2^+$ ion embedded in two interconnected 5-fold rings. Note that a similar bicyclic structure of the $NH_4^+(H_2O)_6$ cluster has been confirmed before.[31] Also, prior diffraction studies[51] of concentrated HCl solutions led to the proposition[52] of a polymeric structure of $HCl(H_2O)_6$ that similarly consists of an $H_5O_2^+$ ion enclosed in the double five-membered rings.

Despite the structural complexity of the octamers, the observed spectrum in Figure 12 matches satisfactorily with the calculated spectrum of isomer **8II**. This is particularly true in the free-OH stretching region where the predicted spectral pattern (both frequencies and intensities) agrees exceptionally well with the observation. We cannot presently draw a definite conclusion that this isomer is solely responsible for the observed spectrum since a large number of low-lying isomers may coexist. However, given the unusually good agreement between calculations and observations, it is suggested that the $H_5O_2^+$-centered isomer (**8II**), which is one of the lowest-energy isomers of $H^+(H_2O)_8$, may prevail in the supersonic expansion.

Discussion

A. $H_5O_2^+$-Containing Clusters. The $H_5O_2^+$-containing water clusters are fundamentally important as prospective proton transfer intermediates. Any insight into their existence helps interpret the anomalously large proton mobility in liquid water and solid ice. In the past three decades, the $H_5O_2^+$ ion and its clusters have only been reported within some inorganic crystals;[25,53] conclusive experimental evidence for their existence in aqueous acids (except concentrated HCl) was not yet

(50) Chang, H.-C.; Wang, Y.-S.; Lee, Y. T.; Chang, H.-C. *Int. J. Mass Spectrom.* **1998**, *180*, 91.

(51) Kameda, Y.; Usuki, T.; Uemura, O. *Bull. Chem. Soc. Jpn.* **1998**, *71*, 1305.

(52) Agmon, N. *J. Phys. Chem. A* **1998**, *102*, 192.

(53) Bell, R. A.; Christoph, G. G.; Fronczek, F. R.; Marsh, R. E. *Science* **1975**, *190*, 151.

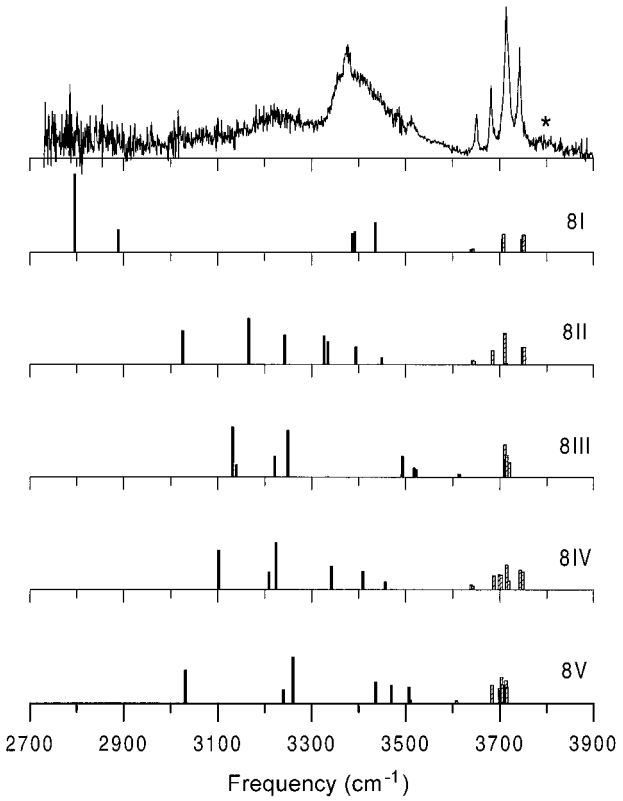

Figure 12. Vibrational predissociation spectrum of $H^+(H_2O)_8$ in the OH stretching region. The beam was expanded at a nozzle temperature of 250 K and a backing pressure of 130 Torr. Shown underneath are the ab initio-calculated stick diagrams of OH stretches for isomers collected in Figure 11. Note that the intensities of free-OH stretches (▨) have been amplified by a factor of 5 for clearer comparison with those of bonded-OH stretches (■). The asterisk denotes H_2O combination bands.[43]

provided.[52,54] In the gas phase, identification of this elusive water cluster was also deemed difficult, primarily because $H_5O_2^+$ can only exist in a symmetric environment. Except for a limited number of isomers with proper symmetries, most of the cluster ions synthesized by a supersonic expansion are H_3O^+-centered. In the present study which combines infrared measurements and ab initio calculations, we have provided compelling spectroscopic and computational evidence for the existence of $H_5O_2^+$ within water clusters in the gas phase. Furthermore, it demonstrates that the $H_5O_2^+$-containing isomers can become more stable than their H_3O^+ counterparts in larger water clusters with a size of $n \geq 6$.

To further investigate the likelihood of $H_5O_2^+$ formation in protonated water clusters, we compare computations using various methods (B3LYP, MP2, and MP4) and basis sets (6-31+G* and aug-cc-pVDZ). All computations in Table 5 agree on the prediction that the $H_5O_2^+$-containing isomers, **6II** and **7VI**, are more strongly bound than other members of the same solvation group. Although the amount of stabilization of the $H_5O_2^+$-centered isomers with respect to the H_3O^+ ones is small and in some cases does not exceed 0.5 kcal/mol, the computed relative energies of the isomers are in support of our spectral assignments. The identification of the $H_5O_2^+$-containing water clusters (**6II**, **7VI**, and possibly **8II**) in this work thus builds on computation and experiment in equal parts.

Being a prospective proton-transfer intermediate,[8−10] isomer **6II** deserves a close examination. Depicted in Figure 13a is the structure of this isomer with an $H_5O_2^+$ ion core fully covered by one layer of water. In this isomer, the four solvent water molecules linked to the ion core are all in the form of 1° H_2O-(A). The fully solvated $H_5O_2^+$ maintains a structure similar to that of the isolated $H_5O_2^+$. The lengths of the two OH bonds involving the excess proton are essentially identical (r_{OH^+} = 1.205 and 1.210 Å by B3LYP/6-31+G*),[29] and the two water molecules in direct contact with the proton lie in two intersected planes, yielding a symmetry of C_2. Owing to this symmetry, the species has a highly simplified OH-stretching spectrum for both the ion core and the solvent molecules. No free-OH stretching absorptions of H_2O(AD) at ~3710 cm^{-1} are present in its spectrum (Figure 6, spectrum **6II**). This spectral characteristic derives naturally from the structure of $H_5O_2^+(H_2O)_4$, which bears close resemblances to the lowest-energy isomer of $NH_4^+(H_2O)_4$,[31,32] as depicted in Figure 13b.

Table 5. Comparison of the Calculated Total Interaction Energies (kcal/mol) of $H^+(H_2O)_n$ Isomers Using Various Computational Levels

	ΔE_n			
isomers[a]	B3LYP/ 6-31+G*	MP2/ 6-31+G*	MP4- (SDQ)[b]	B3LYP/ aug-cc-pVDZ
6I	−93.9	−88.3	−85.3[c]	−91.7
6II	−95.0	−88.8	−85.8[c]	−93.0
6III	−93.6	−88.2		
6IV	−93.6	−88.1		
6V	−93.9	−88.1	−84.6[c]	
6VI	−92.5	−86.5		
7I	−103.7	−97.4	−92.8[d]	
7III	−104.2	−97.8	−93.0[d]	
7VI	−104.9	−98.2	−93.4[d]	
7VII	−102.1	−95.5		
7VIII	−104.0	−97.2		
7IX	−103.2	−96.9		
7X	−103.7	−97.2		

[a] Isomeric structures illustrated in Figures 5 and 8. [b] Using the MP2/6-31+G* geometry. [c] Using the 6-311+G(3df,2p) basis set. [d] Using the 6-31+G* basis set.

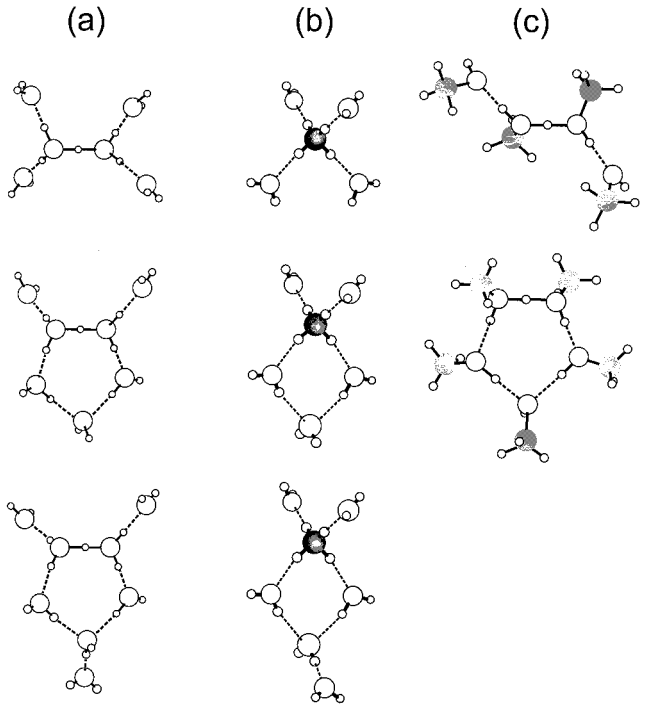

Figure 13. Similarities in the structures of (a) $H_5O_2^+(H_2O)_{4-6}$, (b) $NH_4^+(H_2O)_{4-6}$, and (c) $H^+(CH_3OH)_{4,5}$. The C, N, O, and H atoms are denoted by light and dark gray shaded circles, ○, and ◦, respectively.

(54) Giguère, P. A. *Chem. Phys.* **1981**, *60*, 421. Librovich, N. B.; Sakun, V. P.; Sokolov, N. D. *Chem. Phys.* **1981**, *60*, 425.

The ring-shaped heptamer **7VI** has a structure resembling that of cyclic $H^+(CH_3OH)_5$ [denoted as $C_2H_9O_2^+(CH_3OH)_3$].[33] It consists of a symmetric, but not equilateral, pentagon with an interoxygen distance of 2.418 Å for the shortest side containing the excess proton (Figure 13a,c). Owing to the ring formation, the structure of the $H_5O_2^+$ ion core is slightly twisted with two of the $\angle H-O-H^+$ angles reduced by ~3°.[29] Notably, the general feature of this heptamer is similar to that of the ring-shaped $NH_4^+(H_2O)_5$,[31] except that the ion core is now replaced by $H_5O_2^+$. Figure 13 compares the structures of $H_5O_2^+(H_2O)_5$, $NH_4^+(H_2O)_5$, and $C_2H_9O_2^+(CH_3OH)_3$ to illustrate the similarities between them. The three species all possess one 2° H_2O(AA) [or 2° CH_3OH(AA)] and two 1° H_2O(AD) [or 1° CH_3OH(AD)] molecules. As previously noted for $NH_4^+(H_2O)_5$ [or $C_2H_9O_2^+(CH_3OH)_3$], the bonded-OH stretches of the two coupled 1° H_2O(AD) [or 1° CH_3OH(AD)] oscillators can display a characteristic absorption doublet at ~3550 cm^{-1} (or ~3450 cm^{-1}). The doublets are so well isolated from other lower-frequency bonded-OH stretching modes that they can be clearly identified in the spectra.[55] It has been emphasized and also demonstrated before[33] that this distinct vibrational feature is the fingerprint of a *symmetric*, ring-shaped isomer of protonated water and methanol clusters. This lends further support to the above assignment of the 3544/3555 cm^{-1} doublet to the corresponding modes of isomer **7VI**.

B. Enthalpy versus Entropy Effects. In the aspect of ring formation, the three cluster ions $H^+(H_2O)_n$, $NH_4^+(H_2O)_n$, and $H^+(CH_3OH)_n$ substantially differ. First, a compact four-membered ring with a completely solvated ion core can easily form in $NH_4^+(H_2O)_5$.[31] For H_3O^+, it has one pair of free electrons which does not participate in hydrogen bonding; therefore, one would expect a four-membered ring to form at $m = 4$ of $H_3O^+(H_2O)_m$ as in the case of $CH_3NH_3^+(H_2O)_4$.[50] However, such a ring formation is indiscernible for $H^+(H_2O)_5$ at the cluster temperature of 150−190 K in the present experiment. This is primarily because in $H^+(H_2O)_5$, the ring formation results in a substantial reduction of entropy ($\Delta\Delta S_n \sim -10$ cal/(mol·K) for **5I** → **5III**) and the gain in enthalpy ($\Delta\Delta H_n^{298} \sim 0$ kcal/mol for **5I** → **5III**) owing to additional hydrogen bond formation is insufficient to compensate for the free energy increase due to the entropy loss. The $NH_4^+(H_2O)_5$ stands as an interesting contrast, where the enthalpy difference between the ring-open and ring-closed forms is ~1 kcal/mol which is sufficiently large to allow ring closing at 170 K.[31] We attribute the result of the calculation that ΔE_n(**5I**) < ΔE_n(**5III**) to the wide angle (115°) included by the two interconnected O−H bonds of H_3O^+.[56] The angle is substantially wider than the corresponding angle of 109° for NH_4^+ and 107° for $CH_3NH_3^+$ and does not favor a four-membered-ring formation.[50]

Second, the spectral evidence for the existence of unbranched five-membered rings in $H^+(H_2O)_n$ is lacking. This is in marked contrast to that of $H^+(CH_3OH)_n$, where a compact five-membered ring isomer has been found at $n = 5$.[33] The B3LYP/6-31+G* calculations predict that the five-membered ring is one of the low-energy structures of $H^+(H_2O)_6$; however, it could prevail only when the cluster is cooled to $T_t < 30$ K at which the ring-closed form (**6VII**) is favored over the ring-open form (**6I**) in Gibbs free energies. This can be compared to the transition of the symmetric four-membered ring (**6V**) from **6I**, which occurs at $T_t \sim 70$ K. Unfortunately, for these clusters, the predicted transition temperatures are all too low to be observed in this experiment, disallowing for their identifications at $n = 6$. Only the branched five-membered ring isomers can be experimentally observed, as a result of delicate balancing between enthalpy and entropy effects at the cluster temperature of 170 K.

Predicted by the B3LYP/6-31+G* calculations, the $H_5O_2^+$-centered 5-fold ring isomer, **7VI**, is lowest in both ΔH_n^{298} and ΔG_n^{298} (Table 2). Structural transformation from $H_5O_2^+$-centered to H_3O^+-centered isomers is possible upon raising the beam temperature. We have attempted to observe this transformation by performing temperature-dependence measurements but found nothing dramatic to occur. The failure of this observation can be attributed to the fact that the **7VIII**, **7X** → **7VI** transition involves migration of one water molecule from one corner of the five-membered ring to another. A high barrier must be overcome in the course of the transition, rendering this type of intracluster hydrogen bond rearrangement unavailable.

C. Clustering Kinetics and Photodissociation. In an effort to provide more conclusive experimental evidence for the existence of isomer **6II**, the ion beam was expanded by seeding H_2O in pure Ne.[27,28] Unfortunately, the spectrum obtained for $H^+(H_2O)_6$ in such an expansion resembles that displayed in Figure 6. One can comprehend this result and the small temperature dependence of the spectra in Figure 7 in terms of clustering kinetics. Considering isomers **6I** and **6II**, both of them can be produced by attaching one more H_2O to isomer **5I**. The production of **6II** is less favored probability-wise (1 out of 7) since, to establish the desired clustering, the sixth water molecule must be specifically bound to the H_2O(AD) next to the H_3O^+ ion core. While there is a possibility that the newly formed isomer **6I** can be converted to **6II** via isomer **6IV**, which would effectively lower the barrier, the formation of this intermediate four-membered ring is entropically unfavorable. As a result, the species can be easily trapped in the **6I** configuration upon jet cooling, preventing complete elimination of the vibrational features of this isomer from the spectrum (cf. Figure 7).

A prior experiment[31] demonstrated that the vibrationally induced photodissociation discussed herein involves single photon absorption, although a pulsed infrared laser was used as the light source. The one-photon dissociation is made possible at the expense of internal energy contained in these protonated clusters. Such dissociation should, hence, be better described as a combined event of vibrational predissociation and photoevaporation. In view of its importance in obtaining the infrared action spectra,[31,34] we calculated explicitly the internal energy content of the clusters on the basis of harmonic oscillator approximations and using the frequencies of all vibrational modes provided by the B3LYP/6-31+G* calculations. At the given temperature of 170 K, the clusters are found to accommodate most of their internal energies in the intermolecular vibrational modes with frequency lower than 600 cm^{-1}. A simple estimation from statistical mechanics indicates that isomers **4I**, **5I**, **6I**, **6II**, **7I**, and **7VI** can contain an average internal energy of 1.9, 2.8, 3.6, 3.9, 4.6, and 4.5 kcal/mol, respectively, and the difference in energy among isomers of the same solvation group is less than 0.5 kcal/mol.

Finally, we emphasize that the protonated water clusters can be converted from the $H_5O_2^+$-centered to the H_3O^+-centered forms, or vice versa, by photodissociation. The fragmentation channels, **6II** → **5I** + H_2O and **7II** → **6II** + H_2O, serve as two citable examples. Notably, this interconversion between $H_5O_2^+(H_2O)_{n-2}$ and $H_3O^+(H_2O)_{n-1}$ isomers is analogous to that occurring in liquid water,[8−10] where hydrogen-bond breaking

(55) The vibrations resonant at ~3550 cm^{-1} are similar to those of the bonded-OH stretches of double-donor H_2O molecules in neutral water clusters.[36,60]

(56) Gudeman, C. S.; Saykally, R. J. *Annu. Rev. Phys. Chem.* **1984**, *35*, 387.

is commonly induced by thermal fluctuations with an activation barrier of 2.4 kcal/mol.[57] The presently observed photofragmentation processes can, therefore, be considered as an alternative form of proton transfer activated by vibrational excitation.[33]

Conclusions

This study solves a longstanding enigma[3] concerning the vibrational spectroscopy and structures of protonated water clusters. The success was made possible by performing ab initio calculations and spectroscopic measurements on size-selected water clusters synthesized by a supersonic expansion. A number of characteristic vibrational features in both the free- and hydrogen-bonded-OH stretching regions of the ion core and the solvent water molecules are observed for $H^+(H_2O)_{5-8}$. The investigations allow us to identify the structurally unique $H_5O_2^+$-containing isomers for the first time at both $n = 6$ and 7. Additional structures identified for the protonated water heptamer are five-membered rings which display distinct bonded-OH stretching absorptions at 3500−3600 cm^{-1} for their H_2O(AD) molecules attached to an H_2O(AA). The observation of the free-OH stretch of three-coordinated H_2O also has a significant contribution to the identification of these isomers.

The presently obtained result is a complement to that of neutral water clusters,[58−60] which have been extensively studied for sizes of $n = 2$ up to $n = 10$. In neutral $(H_2O)_n$, a three-dimensional hydrogen-bonding network emerges at $n = 6$,[44] whereas the dominating influence of the extra proton in $H^+(H_2O)_6$ enforces an almost planar noncyclic structure and favors the formation of five-membered rings,[61] instead of four- or six-membered rings, in $H^+(H_2O)_n$ of $n = 7$. This unique feature could be of particular significance in the hydration of biological macromolecules, which are primarily charged, as the formation of pentagonal water clusters has been postulated in a variety of biopolymer crystallites.[62]

Starting with protonated water dimers,[43] we have systematically investigated the infrared spectra of $H^+(H_2O)_n$ as a function of cluster sizes. This series of investigations is expected to help resolve the controversy[54] whether the structure H_3O^+ or $H_5O_2^+$ better describes hydrated protons in aqueous acids. As demonstrated by the present investigations, the excess proton in $H^+(H_2O)_n$ can be either localized on one single water or between two water subunits. Whichever actually occurs depends sensitively on the connectivity and symmetry of the embedding hydrogen-bonded solvent matrix. The $H_5O_2^+$ central ion can indeed survive in a symmetric environment in the gas phase. In liquid phase it certainly plays a role in the course of proton migration as induced by thermal solvent fluctuations.[8] It is hoped that the present observations can lead to a better understanding of the proton-transfer reactions not only in gas-phase water clusters but also in aqueous solutions and in relevant biological systems as well.

Acknowledgment. We thank Noam Agmon for several useful comments about the preprint of this paper. We also thank the second reviewer of this paper for his/her critical comments which make a complete presentation of these results possible. The Chinese Petroleum Corp., the Academia Sinica, and the National Science Council of Taiwan (under Contract No. NSC 88-2113-M-001-026) are acknowledged for financially supporting this research project.

JA990033I

(57) Luz, Z.; Meiboom, S. *J. Am. Chem. Soc.* **1964**, *86*, 4768.
(58) Liu, K.; Cruzan, J. D.; Saykally, R. J. *Science* **1996**, *271*, 929. Liu, K.; Brown, M. G.; Carter, C.; Saykally, R. J.; Gregory, J. K.; Clary, D. C. *Nature* **1996**, *381*, 501.
(59) Huisken, F.; Kaloudis, M.; Kulcke, A. *J. Chem. Phys.* **1996**, *104*, 17.
(60) Buck, U.; Ettischer, I.; Melzer, M.; Buch, V.; Sadlej, J. *Phys. Rev. Lett.* **1998**, *80*, 2578.
(61) The five-membered-ring formation also appeared in the ab initio molecular dynamics simulations of proton transfer in liquid water.[8]
(62) Neidle, S.; Berman, H.; Shieh, H. S. *Nature* **1980**, *288*, 129. Teeter, M. M. *Proc. Natl. Acad. Sci. U.S.A.* **1984**, *81*, 6014.